

<sup>1</sup>Devulal.BM.Siva<sup>2</sup>D. Ravi Kumar<sup>3</sup>

## Design of a Novel Converter Topology for Micro Grid Applications



**Abstract:** - The Renewable Energy Sources (RES) are the primary source of energy because of reduction in fossil fuels day to day. The primary resource in all available non-conventional energy sources is solar energy. Solar energy is obtained normally from Photo Voltaic (PV) cells. In PV cells a photo diode is used which converts the sun irradiation into DC voltage, which is normally a low value, so this is not sufficient to run the electrical loads which are connected to the micro grids. To avoid this problem, a novel boost converter is needed to improve the voltage profile, but it has a problem of high ripple content in voltage profile, which is not preferable for giving as I/P to the Inverter. Normally inverter will take constant DC as an I/p and convert into Alternating Current (AC) voltage. To avoid the above-described ripple, a novel hybrid Pulse Width Modulation (PWM) based DC -DC converter is presented in this paper along with a SPWM inverter circuit which finds its applications in micro grids. The distinctive topologies of 13 and 21 level inverter have been analyzed with reduced number of switches. In traditional topologies a greater number of switches are required, and it can be decreased by planning the diverse topologies. The current distinctive topology is described and compared with the conventional configurations and the corresponding results are presented. With this, it can be observed that the proposed topology gives the better outcomes. This can be utilized as a part of various micro grid inverter applications.

**Keywords:** Renewable Energy Sources (RES), Photo Voltaic (PV), Total Harmonic Distortion (THD), Pulse Width Modulation (PWM), Cascaded H-Bridge (CHB), Input(I/P), Output(O/P).

### I. INTRODUCTION

In current days, principal job in power age is with sustainable renewable energy power Sources (RES) on account of decrease in the petroleum derivatives ordinarily goes about as the primary part of all promptly accessible non-regular energy sources. Energy is a fundamental element for the working and financial improvement of the industrialized world. Energy has become basic component for the progressive financial thriving. The energy utilization process again needs either DC-AC transformation or AC-DC change. The DC-AC change finds its significant application in continuous uninterrupted power supply (UPS) and Renewable Energy (RE). To supply during blackouts, most UPS frameworks use batteries, as a rule lead corrosive, as capacity instrument. The battery should give the reinforcement without the lattice supply. Be that as it may, the voltage given by the battery alone may not be sufficient to give the reinforcement. Right away, the battery O/P power which is DC should be changed over completely to AC with the assistance of an inverter. Evidently, the O/P of inverter should be move forward with the assistance of move forward transformer to accomplish an O/P of 220V, 50Hz [1]. An elective way to deal with a similar interaction is by utilizing a power electronic converter called DC support converter. The support converters are utilized in numerous applications, including photovoltaic frameworks, UPS, and Energy Component (FC) frameworks [1].

The standard DC support converter can't give a high increase, when the voltage gain is high the proficiency of lift converter lessens. The explanation being the misfortunes in the natural resistors of the converter increment

---

<sup>1</sup>Corresponding author: B. Devulal,

<sup>1</sup>Dept. of Electrical and Electronics Engineering, Research Scholar, Annamalai University, Chidambaram, Tamil Nadu, India. E-mail: devulalb@gmail.com

<sup>2</sup>Dept. of Electrical and Electronics Engineering, Assistant Professor, Annamalai University, Chidambaram, Tamil Nadu, India. E-mail: vasi.siva@gmail.com

<sup>3</sup>Dept. of Electrical and Electronics Engineering, Associate Professor, VNR Vignana Jyothi Institute of Engineering and Technology, Hyderabad, Telangana, India. E-mail: ravikumar\_d@vnrvjiet.in

when the obligation cycle expands, this compromises the presentation of the converter [2],[3]. To defeat this constraint, high addition converter can be utilized to accomplish higher increase [4],[5]. AC O/P can be accomplished with the assistance of inverter. Likewise, DC-AC transformation tracks down its application in RES frameworks. In such applications like sunlight based Photograph Voltaic (PV) frameworks, the DC O/P power from PV should be switched over completely to AC power [6],[7]. An Inverter circuit is utilized in overflow with a clever Heartbeat Width Tweak DC half breed converter [8]-[14]. In general, when 's' number of Direct Current (DC) inputs are considered, the number of levels is  $2S+1$ . The state of the art PWM DC mixture converter is basically used to upgrade the PV cell voltage profile and arrive at the essential I/p voltage level for an Inverter circuit that is introduced in single stage 13 and 21-level MLIs. The 21-levels of O/P through 10 H-cells utilizes power for miniature framework applications.

II. NOVEL DC-DC HYBRID CONVERTER USING PWM

Fig.1 shows the schematic for a Novel DC-DC hybrid converter that uses Pulse width Modulation (PWM). Phase-shifted switching operation based on PWM technique is used to energize the combination of two anti-parallel connected inductors, which are used to connect the DC-DC hybrid converter. Fig.2 shows the PWM switching sequence diagram of the phase shifting operation. In this phase shifting operation, the phase difference between two hybrid switches is  $180^\circ$ .

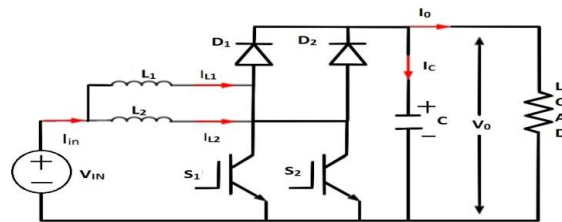


Figure 1 Novel Pulse Width Modulation based DC-DC hybrid converter

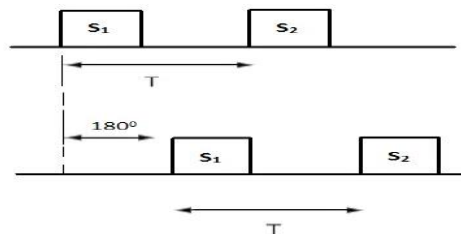


Figure 2 PWM switching sequence diagram of the phase shifting operation techniques

In the mentioned Novel PWM based DC-DC hybrid converter, two inductors  $L_1$  and  $L_2$  are selected with an equal value and is equivalent to  $L$  for the equation analysis purpose. The Duty ratio of  $S_1$  was considered as  $D_1$  similarly for  $S_2$  it is  $D_2$ . The duty ratio values of both operated switches ( $S_1$  and  $S_2$ ) were considered as  $D$ .

The Novel PWM DC-DC hybrid converter can operate in the following modes.

Mode I: When switch  $S_1$  is ON (closed) and  $S_2$  is OFF (opened) at time  $T_0$ , the inductor  $L_1$  current begins to rise as it is discharged through the inductor  $L_2$ .

Mode II: When switches  $S_1$  and  $S_2$  are ON (closed) at time  $T_1$ , the inductor  $L_1$  current begins to discharge with the assistance of inductor  $L_2$  and the load.

Mode III: When switch  $S_2$  is OFF (open) and switch  $S_1$  is ON (closed) at time  $T_2$ , the Inductor  $L_2$  current begins to rise while being discharged through the inductor  $L_1$ .

Mode IV: In the same way as in mode II, when switches  $S_1$  and  $S_2$  are OFF (opened) at time  $T_3$ , the inductor  $L_1$  current discharges through inductor  $L_2$  and the load.

III. DESIGN MODEL OF A NOVEL PULSE WIDTH MODULATION (PWM) BASED DC-DC HYBRID CONVERTER

Fig.3 shows the design of a PWM-based DC-DC hybrid converter. Fig.4 & Fig.5 Show various operating modes with  $S_1$  and  $S_2$  ON respectively.

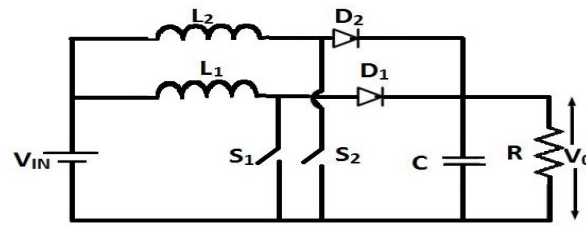


Figure 3 Novel Pulse Width Modulation (PWM) based DC-DC hybrid converter

A. DURING  $S_1$  ON &  $S_2$  OFF

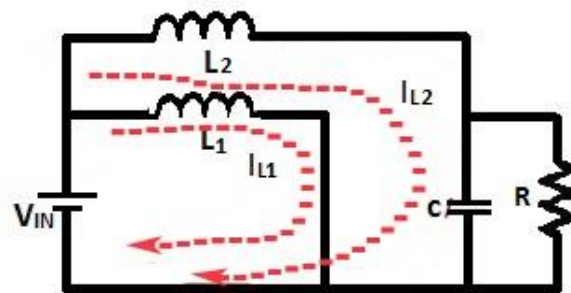


Figure 4 Novel Pulse width Modulation (PWM) based DC-DC hybrid converter with  $S_1$  ON

Voltage across inductor  $L_1$

$$V_{in} = L_1 \frac{dI_1}{dt}$$

Voltage across inductor  $L_2$

$$V_{in} - V_0 = L_2 \frac{dI_2}{dt}$$

Assume  $\Delta I = I_2 - I_1$

$$V_{in} = L_1 \frac{\Delta I}{t_1}$$

$$t_1 = \frac{L \times \Delta I}{V_{in}} \tag{1}$$

B. DURING  $S_1$  OFF &  $S_2$  ON

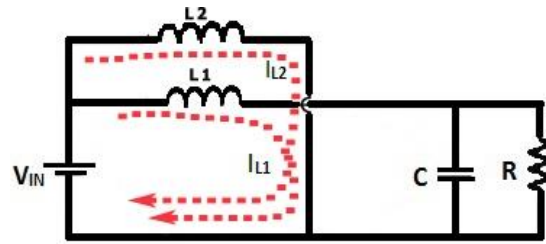


Figure 5 PWM based DC-DC boost converter with S<sub>2</sub> ON

For inductor L<sub>1</sub>

$$V_{in} - V_0 = -L_1 \frac{dI}{dt}$$

$$t_2 = \frac{\Delta I L_1}{V_0 - V_{in}} \quad (2)$$

Substitute t<sub>1</sub>=DT<sub>s</sub> and t<sub>2</sub>=(1-D) T<sub>s</sub>

$$\Delta I = \frac{V_{in} \times t_1}{L}$$

$$\Delta I = \frac{V_0 - V_{in} \times t_2}{L}$$

$$\frac{V_{in} \times DT_s}{L} = \frac{(V_0 - V_{in})}{L} (1 - D)T_s$$

$$\frac{V_0}{V_{in}} = \frac{1}{1-D} \quad (3)$$

Total time period

$$T = t_1 + t_2 = \frac{\Delta I L}{V_{in}} + \frac{\Delta I L}{V_0 - V_{in}}$$

$$T = \frac{\Delta I L V_0}{V_{in}(V_0 - V_{in})} \quad (4)$$

Peak to peak ripple current

$$T = \frac{1}{f}$$

$$\Delta I = \frac{V_{in}(V_0 - V_{in})}{f L V_0} \quad (5)$$

$$\Delta I = \frac{V_{in} * D}{f L} \quad (6)$$

ΔI Indicates ripple flow current and is given in Eqn. (6). It depends on the inductance and duty ratio. Fig.6 shows the voltage and current waveforms across inductors L<sub>1</sub> and L<sub>2</sub>.

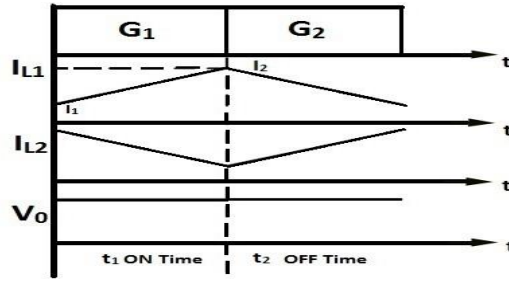


Figure 6 Inductor current and voltage waveforms.

For O/P capacitor

$$\Delta V_c = V_c - V_c(t = 0) = \frac{1}{c} \int_0^{t_1} I_c dt$$

$$= \frac{I t_1}{c}$$

Substituting

$$t_1 = \frac{(V_0 - V_{in})}{V_0 f}$$

$$\Delta V_c = \frac{I_0 D}{f c} \tag{7}$$

The ripple voltage of a capacitor is represented by Eqn. (7), and it depends on the duty ratio as well as capacitance values. Critical case ripple scenario for CCM operation is  $\Delta I = 2I_L$

$$\Delta I = \frac{V_{in} D}{f L} = 2I_L = 2I_0 = 2 \times \frac{V_0}{R}$$

$$= \frac{2 \times V_{in}}{(1 - D) R}$$

$$L_{critical} = \frac{D(1 - D) R}{2 f} \tag{8}$$

The critical case ripple for capacitor

$$\Delta V_c = 2V_0$$

$$2V_0 = \frac{I_0 D}{f c} = 2I_0 R$$

$$C_{critical} = \frac{D}{2 f R} \tag{9}$$

The specifications of a novel PWM-based DC-DC hybrid converter coupled to an induction drive are given in Table.1

Table.1 Parameters

S.No	Parameter	Value
1	V <sub>in</sub>	230V
2	L	3.5mH
3	C	250μF
4	R	18Ω
5	A	62.5%
6	R <sub>s</sub>	2.950Ω
7	L <sub>s</sub>	7.5mH

C. SIMULINK MODEL OF A NORMAL PWM BASED DC-DC HYBRID CONVERTER

The simulation model of a Normal PWM-based DC-DC Converter is depicted in Fig.7. In this scenario, a DC supply is provided as I/P to a regular converter so that the O/P voltage is increased. To obtain pulses for the gate in this, only one switch is used. The wave form for current passing through the inductor is shown in Fig.8.

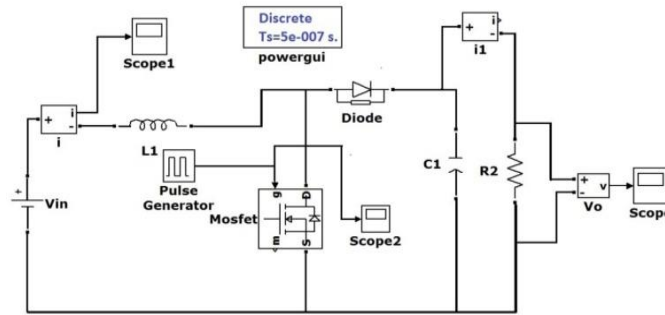


Figure 7 Normal PWM based DC-DC converter

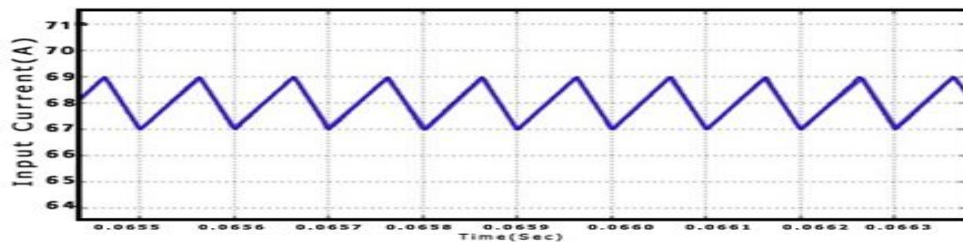


Figure 8 Current passing through inductor

The O/P voltage wave shape and switching pulse with a duty Ratio of 62.5% are depicted in Fig.9 and 10. The resultant voltage's magnified value is shown in Fig.11, However, the presence of ripple in the Normal PWM-based DC-DC converter resulting voltage is readily seen in the zoomed result.

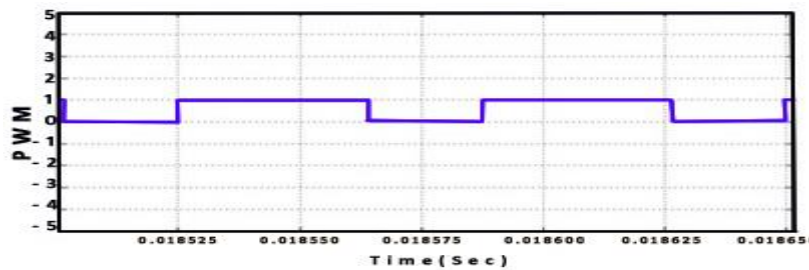


Figure .9 Switching pulse

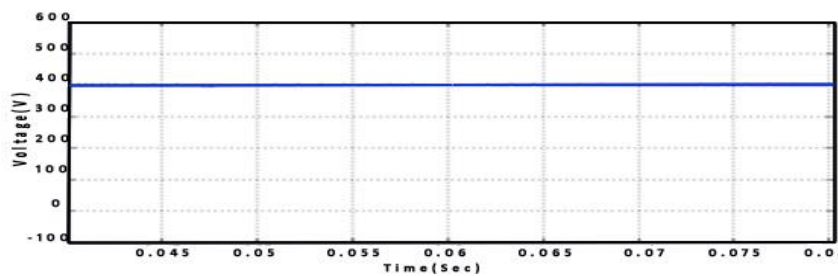


Figure 10 Converter DC O/P voltage Waveform

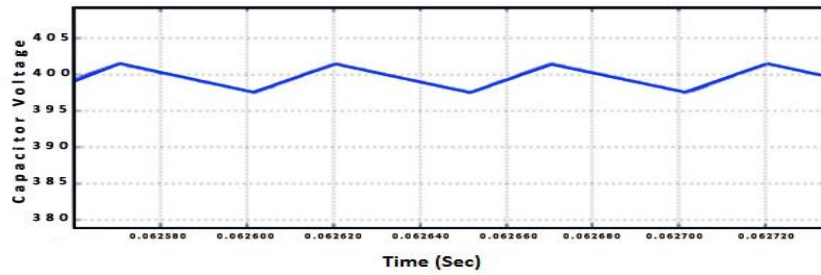


Figure 11 Voltage across capacitor

D. SIMULINK MODAL A NOVEL PWM BASED DC-DC HYBRID CONVERTER

Using a novel PWM-based DC-DC hybrid converter with two identical switches, as shown in Fig.12, it is possible to reduce the O/P ripples in the conventional DC-DC converter.

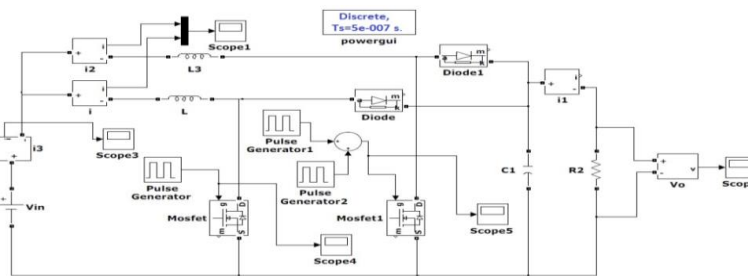


Figure.12 Simulink model for novel PWM based DC-DC hybrid Converter

Switching signals to the two switches are displaced by  $180^\circ$  in this converter. The I/P current wave form with hybrid converter is shown in Fig.13 and it can be seen that there is less ripple content in the current than with a conventional DC-DC converter. The ripple content in this converter is limited to less than 1A, whereas with normal converter it is 2A. The current passing through inductors  $L_1$  and  $L_2$  are shown in Fig.14. The waveforms for switching pulse are given in Fig.15 and 16 have a  $180^\circ$  phase shift.

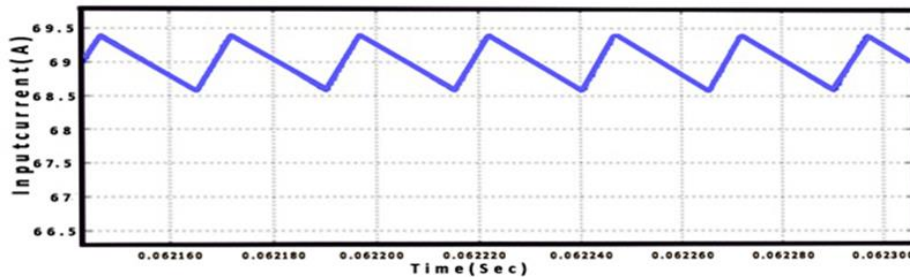


Figure.13 Waveform for I/P current

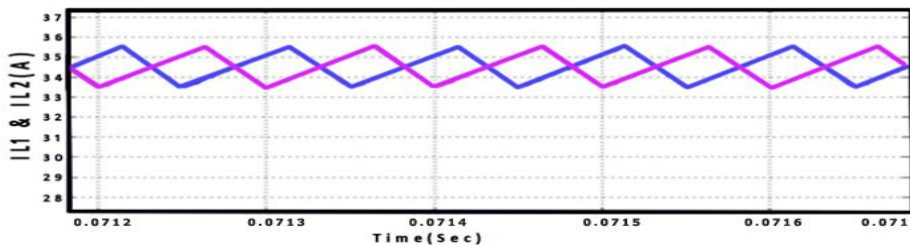


Figure.14 waveforms for inductor currents ( $IL_1$  &  $IL_2$ )

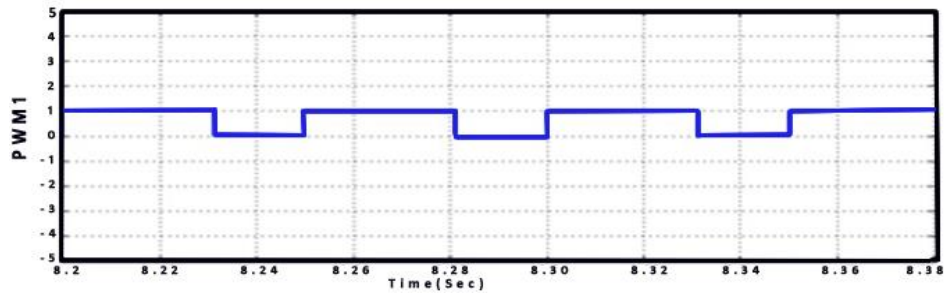


Figure.15 Switching pulse, S<sub>1</sub>

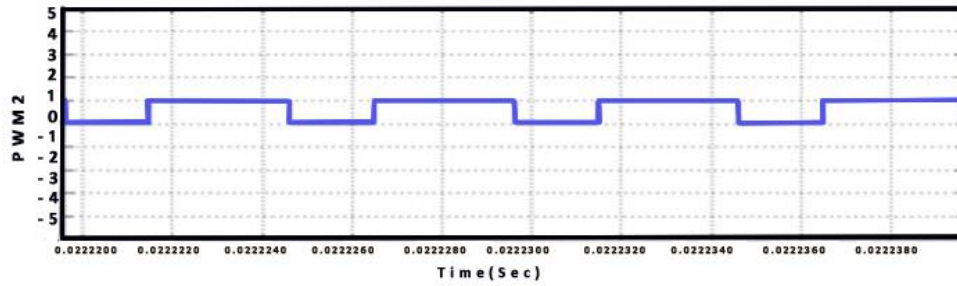


Figure.16 Switching pulse, S<sub>2</sub>

The O/P voltage and voltage across the hybrid converter are given in Fig.17 & 18. The ripple voltage values with hybrid converter is very less i.e 0.8 Vp-p where as in normal DC-DC converter it is 5 Vp-p

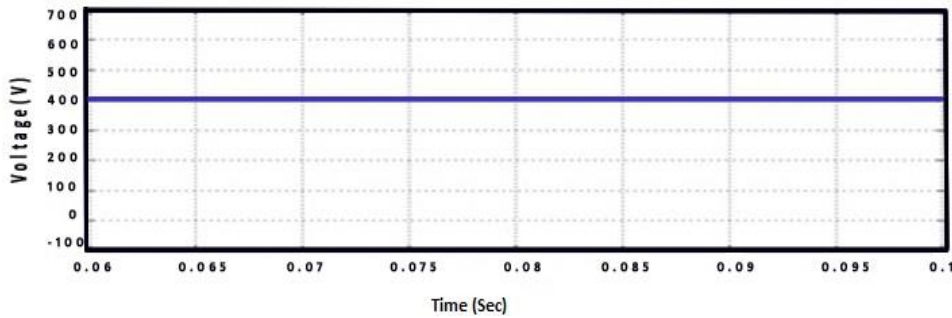


Figure.17 Converter DC O/P voltage wave form

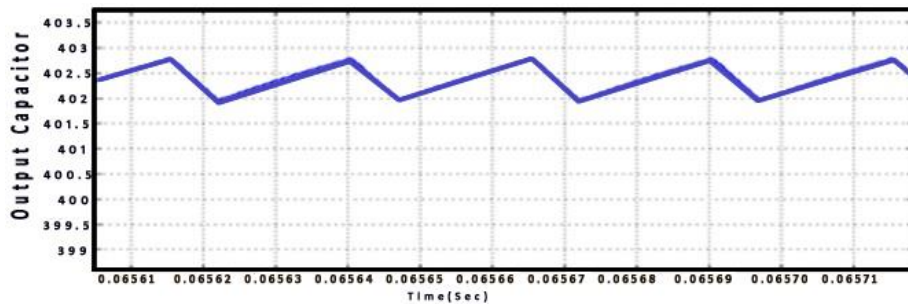


Figure.18 Waveforms for voltage across capacitor



IV. 11-LEVEL CHB BLOCK DIAGRAM MULTI LEVEL INVERTER TOPOLOGY

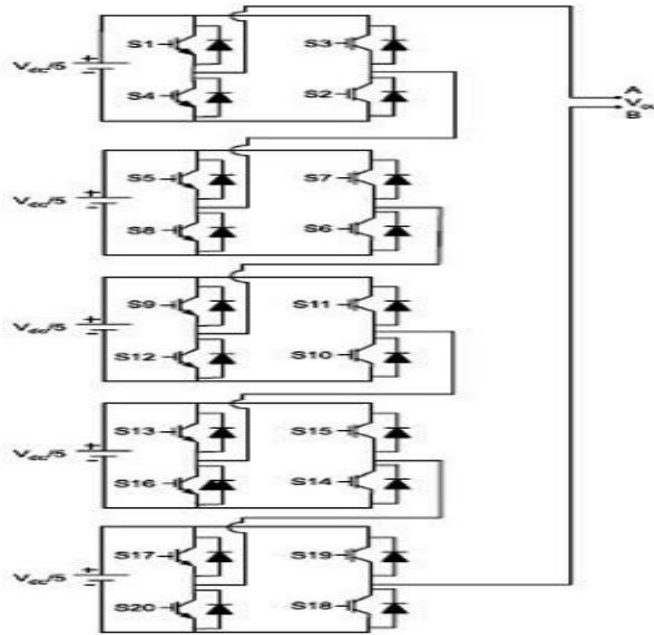


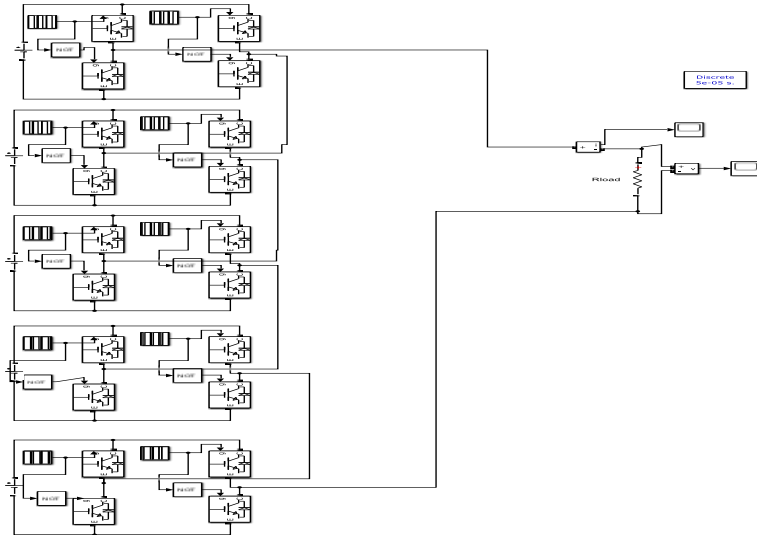
Fig.19 Schematic diagram for a 11-level CHB Inverter Topology

Table 2: Switching of a 11-level CHB converter

Voltage Level	Switching Operation																			
	S <sub>1</sub>	S <sub>2</sub>	S <sub>3</sub>	S <sub>4</sub>	S <sub>5</sub>	S <sub>6</sub>	S <sub>7</sub>	S <sub>8</sub>	S <sub>9</sub>	S <sub>10</sub>	S <sub>11</sub>	S <sub>12</sub>	S <sub>13</sub>	S <sub>14</sub>	S <sub>15</sub>	S <sub>16</sub>	S <sub>17</sub>	S <sub>18</sub>	S <sub>19</sub>	S <sub>20</sub>
0	0	1	0	1	0	1	0	1	0	1	0	1	0	1	0	1	0	1	0	1
V <sub>dc</sub> /5	1	1	0	0	0	0	0	0	0	0	0	0	0	0	0	0	0	0	0	0
2V <sub>dc</sub> /5	0	0	0	0	1	1	0	0	0	0	0	0	0	0	0	0	0	0	0	0
3V <sub>dc</sub> /2	1	1	0	0	1	1	0	0	1	1	0	0	0	0	0	0	0	0	0	0
4V <sub>dc</sub> /5	1	1	0	0	1	1	0	0	1	1	0	0	1	1	0	0	0	0	0	0
V <sub>dc</sub>	1	1	0	0	1	1	0	0	1	1	0	0	1	1	0	0	1	1	0	0
-V <sub>dc</sub> /5	0	0	1	1	0	0	0	0	0	0	0	0	0	0	0	0	0	0	0	0
-2V <sub>dc</sub> /5	0	0	1	1	0	0	1	1	0	0	0	0	0	0	0	0	0	0	0	0
-3V <sub>dc</sub> /5	0	0	1	1	0	0	1	1	0	0	1	1	0	0	0	0	0	0	0	0
-4V <sub>dc</sub> /5	0	0	1	1	0	0	1	1	0	0	1	1	0	0	1	1	0	0	0	0
-V <sub>dc</sub>	0	0	1	1	0	0	1	1	0	0	1	1	0	0	0	0	0	0	1	1

From the above geography it may be affirmed that with an expansion in degree of voltage the expected number of switches is expanding which additionally builds the exchanging misfortunes, cost and intricacy of the circuit and calculation for controlling the switches. To keep away from the above disadvantages, seeing an original inverter geography with a decreased number of switches for miniature framework applications is proposed.

A. MATLAB/SIMULINK MODEL FOR 11-LEVEL CHB INVERTER FED TO R-LOAD



**Figure 20 Schematic diagram for a 11-level CHB Inverter Topology**

Fig.20 represents, 11-level topology for a CHB inverter. In this circuit, a total of 20 switches are used, to get the 11-level single phase O/P voltage & current wave form and FFT analysis are shown in Fig.21,22 & 23.

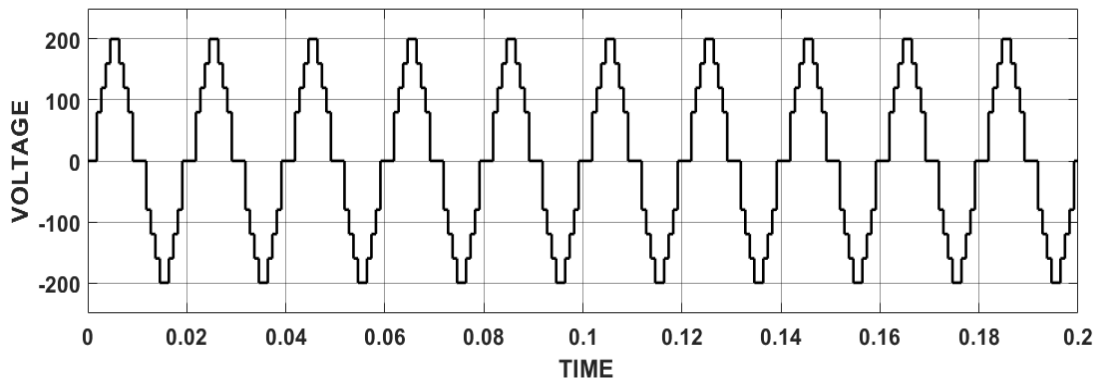


**Figure 21 Voltage wave form of 11-level CHB inverter**

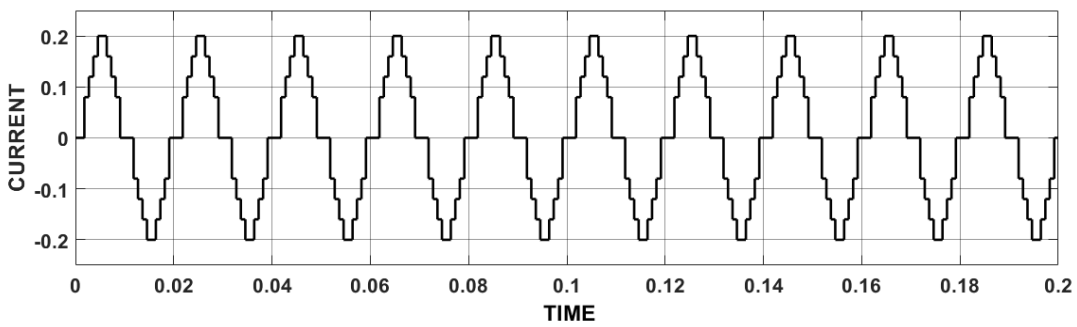


**Figure 22 Current waveform of 11-level CHB inverter**

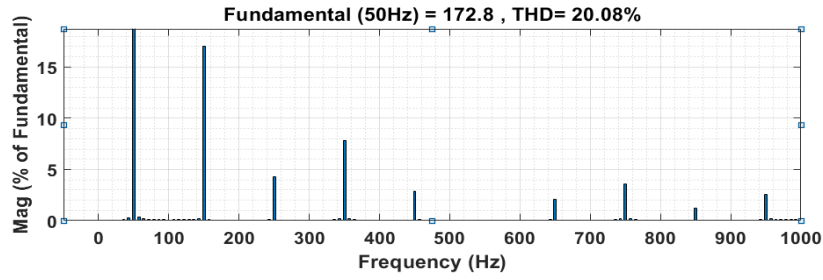


Figure 23 FFT Analysis for 11-level CHB inverter

V. 13-LEVEL CHB BLOCK DIAGRAM MULTI LEVEL INVERTER TOPOLOGY

Fig.24 represents the circuit topology for 13-level CHB inverter and also the respective switching sequence is given in Table 3.

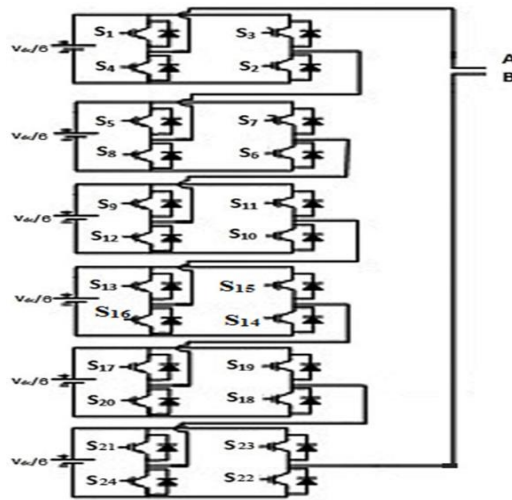


Fig.24 Schematic diagram for a 13-level CHB Inverter

Table 3: Switching of a 13-level CHB Inverter

Voltage Level	Switching Sequence																							
	S <sub>1</sub>	S <sub>2</sub>	S <sub>3</sub>	S <sub>4</sub>	S <sub>5</sub>	S <sub>6</sub>	S <sub>7</sub>	S <sub>8</sub>	S <sub>9</sub>	S <sub>10</sub>	S <sub>11</sub>	S <sub>12</sub>	S <sub>13</sub>	S <sub>14</sub>	S <sub>15</sub>	S <sub>16</sub>	S <sub>17</sub>	S <sub>18</sub>	S <sub>19</sub>	S <sub>20</sub>	S <sub>21</sub>	S <sub>22</sub>	S <sub>23</sub>	S <sub>24</sub>
0	1	1	0	1	0	1	0	1	0	1	0	1	0	1	0	1	0	1	0	1	0	1	0	1
$V_{dc}/6$	1	0	0	1	0	1	0	1	0	1	0	1	0	1	0	1	0	1	0	1	0	1	0	1
$V_{dc}/3$	1	0	0	1	1	0	0	1	0	1	0	1	0	1	0	1	0	1	0	1	0	1	0	1
$V_{dc}/2$	1	0	0	1	1	0	0	1	1	0	0	1	0	1	0	1	0	1	0	1	0	1	0	1
$2V_{dc}/3$	1	0	0	1	1	0	0	1	1	0	0	1	1	0	0	1	0	1	0	1	0	1	0	1
$5V_{dc}/6$	1	0	0	1	1	0	0	1	1	0	0	1	1	0	0	1	1	0	0	1	0	0	1	0
$V_{dc}$	1	0	0	1	1	0	0	1	1	0	0	1	1	0	0	1	1	0	0	1	1	0	0	1
$-V_{dc}/6$	0	1	1	0	1	0	1	0	1	0	1	0	1	0	1	0	1	0	1	0	1	0	1	0
$-V_{dc}/3$	0	1	1	0	0	1	1	0	1	0	1	0	1	0	1	0	1	0	1	0	1	0	1	0
$-V_{dc}/2$	0	1	1	0	0	1	1	0	0	1	1	0	1	0	1	0	1	0	1	0	1	0	1	0
$-2V_{dc}/3$	0	1	1	0	0	1	1	0	0	1	1	0	0	1	1	0	1	0	1	0	1	0	1	0
$-5V_{dc}/6$	0	1	1	0	0	1	1	0	0	1	1	0	0	1	1	0	0	1	1	0	0	1	1	0
$-V_{dc}$	0	1	1	0	0	1	1	0	0	1	1	0	0	1	1	0	0	1	1	0	0	1	1	0

A. MATLAB/SIMULINK MODEL FOR 13-LEVEL CHB INVERTER FED TO R-LOAD

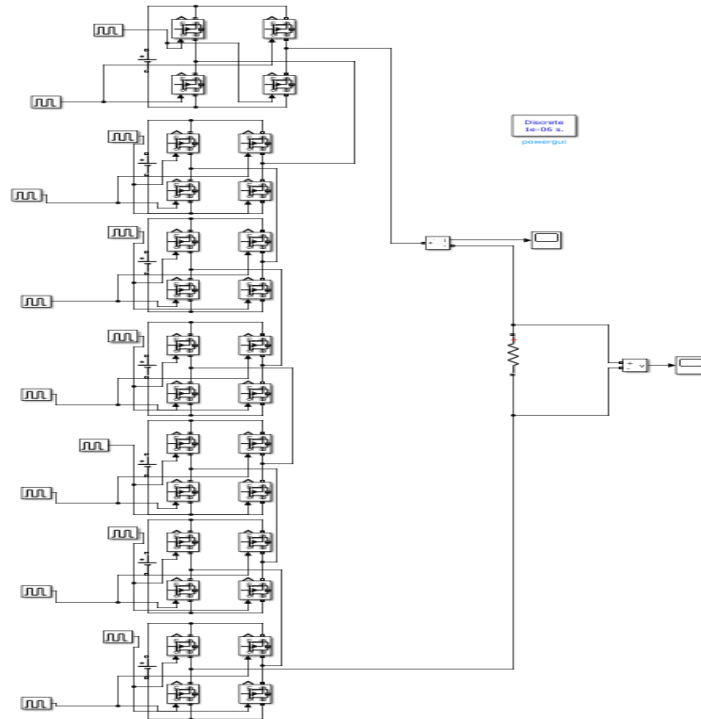


Figure 25 Schematic diagram for a 13-level CHB Inverter Topology

Fig. 25 represents a 13-level topology for a CHB inverter. In the above circuit a total of 24 switches are used to get 13-level, single phase O/P voltage & current wave forms and FFT analysis are given in Fig.26,27&28.

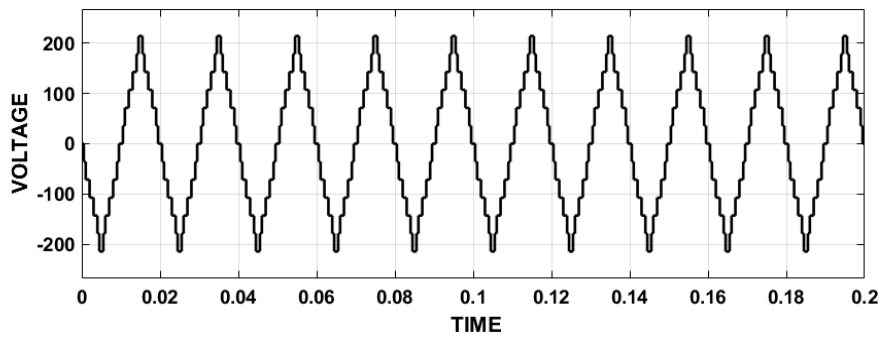


Figure 26 Voltage wave form of 13-level CHB inverter

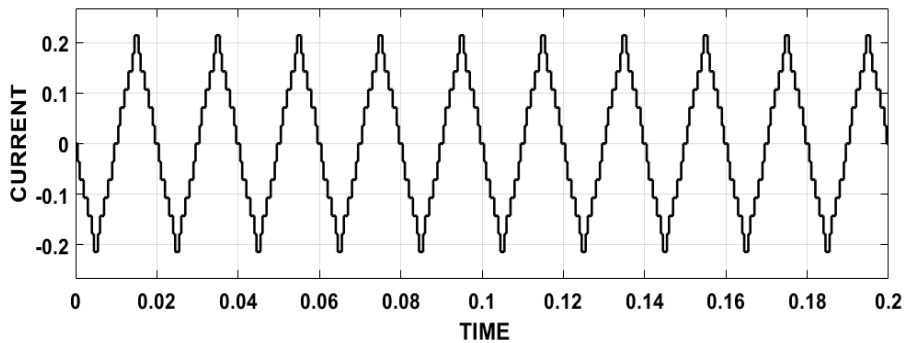


Figure 27 Current waveform of 13-level CHB inverter

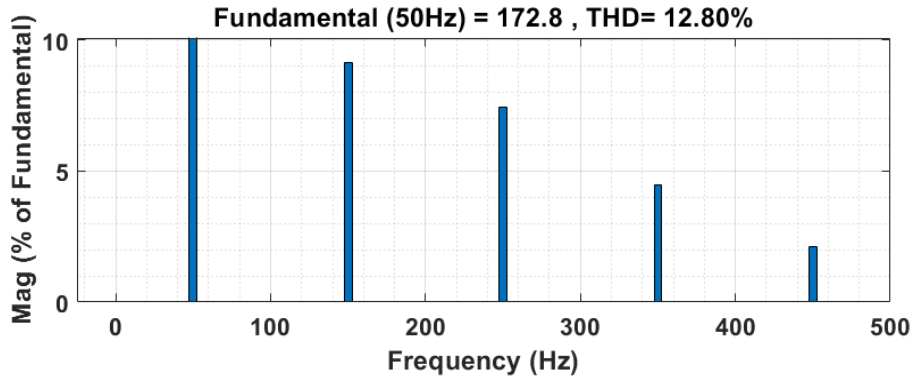


Figure 28 FFT Analysis for 13-level CHB inverter

VI. 21-LEVEL CHB MULTI LEVEL INVERTER TOPOLOGY

The block diagram of Conventional Single Phase 21- level CHB Multilevel Inverter is shown in Fig. 29.

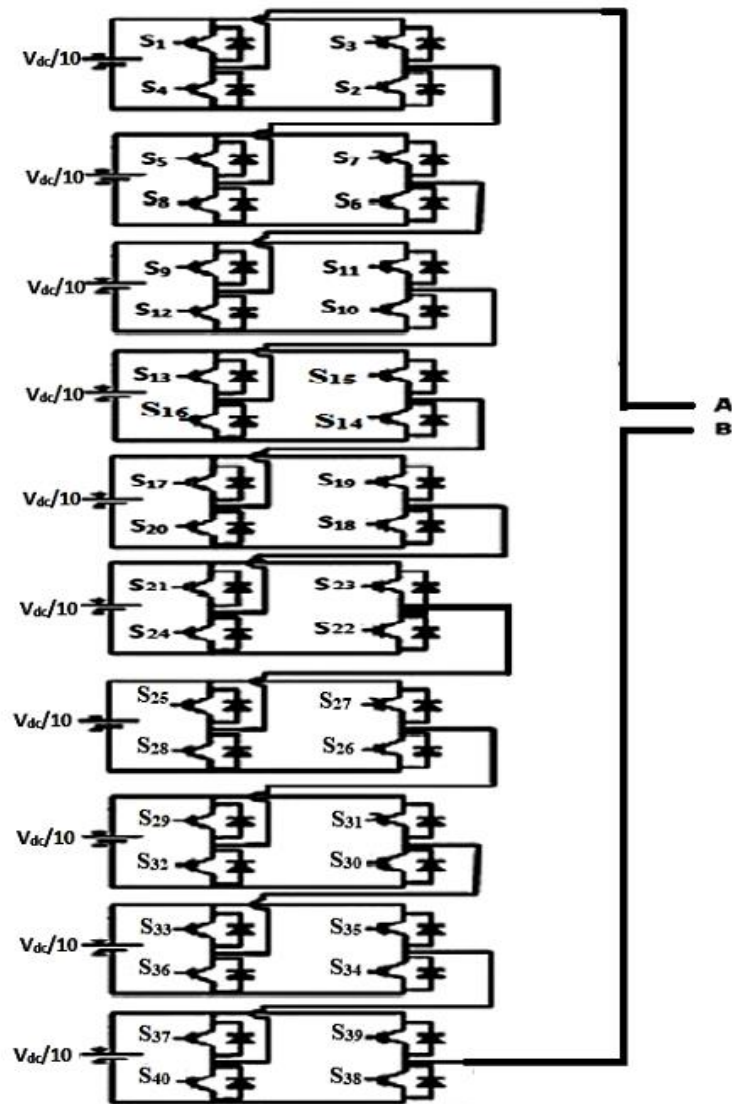


Figure 29 Conventional Single Phase 21-level CHB inverter.

**Table 4: Switching of a 21-level CHB Inverter**

1	0	1	2	3	4	5	6	7	8	9	10	11	12	13	14	15	16	17	18	19	20	21	22	23	24	25	26	27	28	29	30	31	32	33	34	35	36	37	38	39				
2	0	10	20	30	40	50	60	70	80	90	100	90	80	70	60	50	40	30	20	10	0	-10	-20	-30	-40	-50	-60	-70	-80	-90	-100	-90	-80	-70	-60	-50	-40	-30	-20	-10				
3	1	1	1	1	1	1	1	1	1	1	1	1	1	1	1	1	1	1	1	1	0	1	1	1	0	1	1	0	1	0	1	0	1	1	0	1	1	0	1	1	0			
4	2	1	0	1	1	1	0	1	1	0	1	0	1	0	1	1	0	1	1	0	1	1	1	1	1	1	1	1	1	1	1	1	1	1	1	1	1	1	1	1	1	1		
5	3	0	0	0	0	0	0	0	0	0	0	0	0	0	0	0	0	0	0	0	1	0	0	0	1	0	0	1	0	0	1	0	1	0	1	0	0	1	0	0	0	1		
6	4	0	1	0	0	1	0	0	1	0	1	0	1	0	0	1	0	0	1	0	0	0	0	0	0	0	0	0	0	0	0	0	0	0	0	0	0	0	0	0	0	0	0	
7	5	1	1	1	1	1	1	1	1	1	1	1	1	1	1	1	1	1	1	1	1	0	1	1	1	0	1	1	0	1	1	0	0	0	1	1	0	1	1	1	0	1		
8	6	1	0	1	1	1	0	1	1	0	0	1	0	1	1	0	1	1	0	1	1	1	1	1	1	1	1	1	1	1	1	1	1	1	1	1	1	1	1	1	1	1	1	
9	7	0	0	0	0	0	0	0	0	0	0	0	0	0	0	0	0	0	0	0	0	1	0	0	0	1	0	0	1	0	0	1	1	1	0	0	1	0	0	0	1	0		
10	8	0	1	0	0	1	0	0	1	1	1	0	0	1	0	0	0	1	0	0	0	0	0	0	0	0	0	0	0	0	0	0	0	0	0	0	0	0	0	0	0	0	0	
11	9	1	1	1	1	1	1	1	1	1	1	1	1	1	1	1	1	1	1	1	1	0	1	1	1	0	0	0	0	0	0	0	0	0	0	0	1	1	1	0	1	1		
12	10	1	1	0	1	1	1	0	0	0	0	0	0	1	1	0	1	1	1	1	1	1	1	1	1	1	1	1	1	1	1	1	1	1	1	1	1	1	1	1	1	1	1	
13	11	0	0	0	0	0	0	0	0	0	0	0	0	0	0	0	0	0	0	0	0	0	1	0	0	0	1	1	1	1	1	1	1	1	1	1	0	0	0	1	0	0		
14	12	0	0	1	0	0	0	1	1	1	1	1	1	1	0	0	0	1	0	0	0	0	0	0	0	0	0	0	0	0	0	0	0	0	0	0	0	0	0	0	0	0	0	
15	13	1	1	1	1	1	1	1	1	1	1	1	1	1	1	1	1	1	1	1	1	1	1	0	0	0	0	0	0	0	0	0	0	0	0	0	0	0	0	0	0	1	1	1
16	14	1	1	1	0	0	0	0	0	0	0	0	0	0	0	0	0	1	1	1	1	1	1	1	1	1	1	1	1	1	1	1	1	1	1	1	1	1	1	1	1	1	1	1
17	15	0	0	0	0	0	0	0	0	0	0	0	0	0	0	0	0	0	0	0	0	0	0	0	0	1	1	1	1	1	1	1	1	1	1	1	1	1	1	1	1	0	0	0
18	16	0	0	0	1	1	1	1	1	1	1	1	1	1	1	0	0	0	0	0	0	0	0	0	0	0	0	0	0	0	0	0	0	0	0	0	0	0	0	0	0	0	0	0

Table 4 gives 21 level CHB Inverter with 21 different voltage O/P levels with an appropriate control scheme of the switches. The sum of different individual H-bridge inverter O/Ps connected in series is synthesized to get the final sinusoidal O/P voltage for the multilevel inverter.

*A. MATLAB /SIMULINK MODEL FOR A NOVEL PV BASED 21-LEVEL CHB INVERTER*

Fig.30 represents a 21-level topology for a CHB, a total of 40 switches are used to get 21-level single phase O/P voltage and current wave and FFT analysis are given in Fig.31,32 & 33.

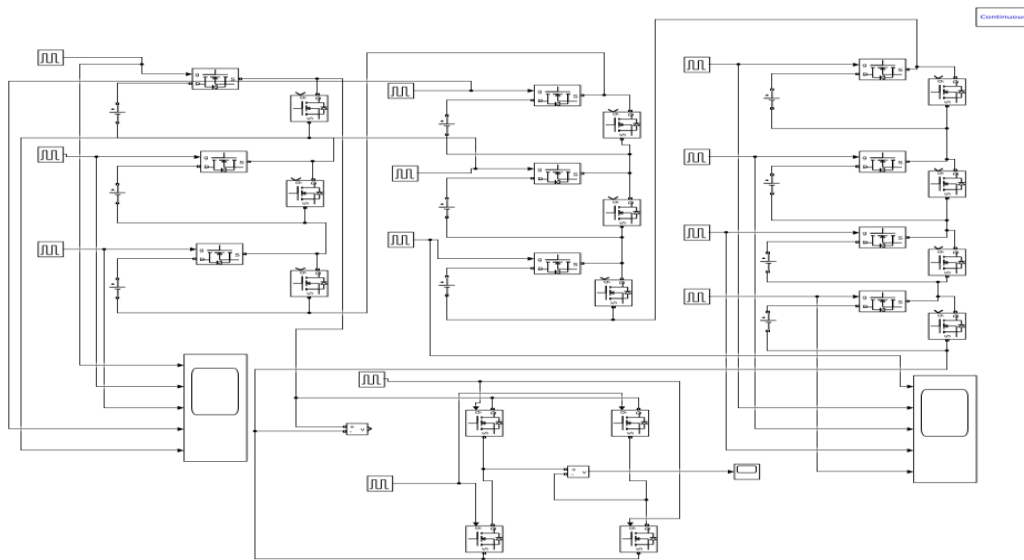


**Figure 30 Schematic diagram for a 21-level CHB Inverter Topology**

Fig. 30 represents a 21-level topology for a CHB inverter. In the above circuit a total of 13 switches are used to get 21-level, single phase O/P voltage & current wave forms and FFT analysis are given in Fig.31,32&33.

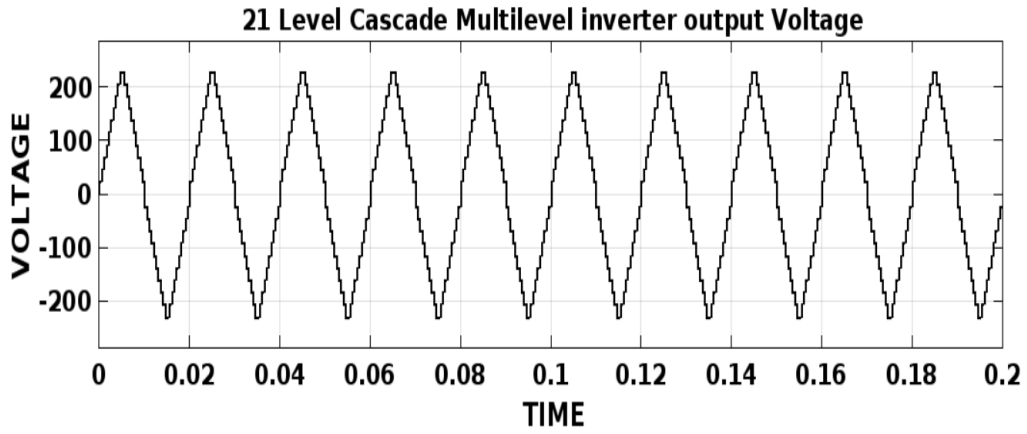


Fig.31 Voltage wave form of 21-level CHB inverter

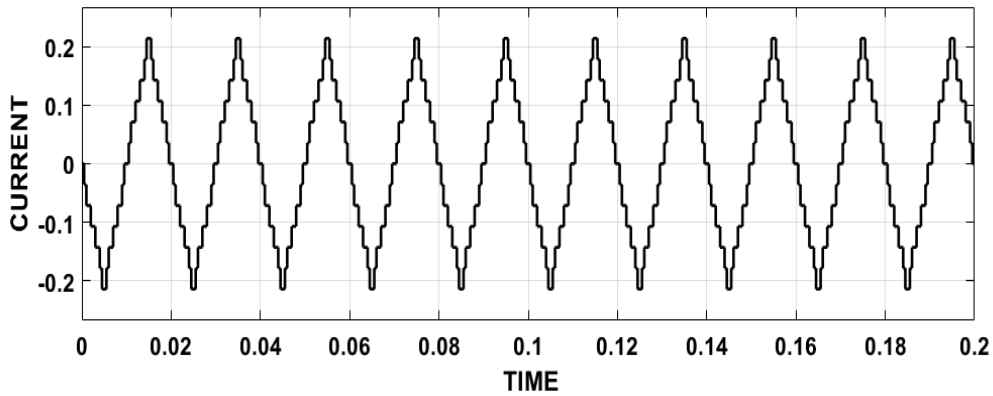


Fig.32 current wave form of 21-level CHB inverter

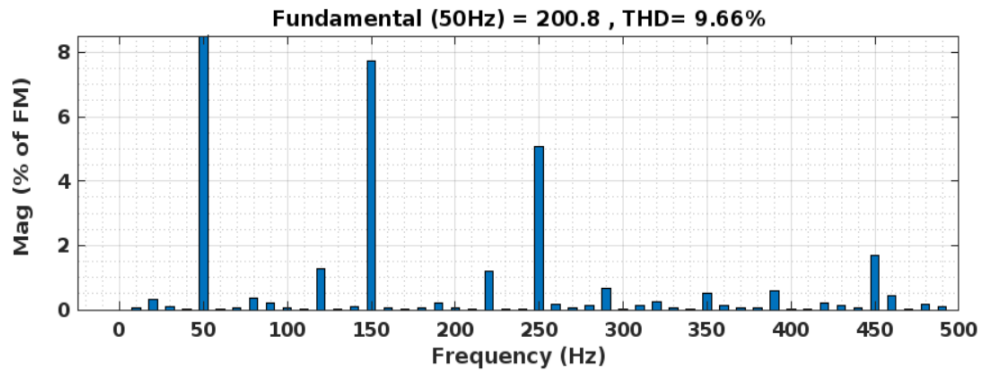


Fig.33 FFT analysis for 21-level CHB inverter

VII. A NOVEL PV BASED SINGLE PHASE 13-LEVEL HYBRID H-BRIDGE INVERTER FED TO R- LOAD

The system block diagram for a Novel PV based Single phase 13-level Hybrid H-Bridge inverter fed to R-load is shown in Fig.34. It represents the complete schematic structure of micro grid operation.

### BASIC SYSTEM Block Diagram

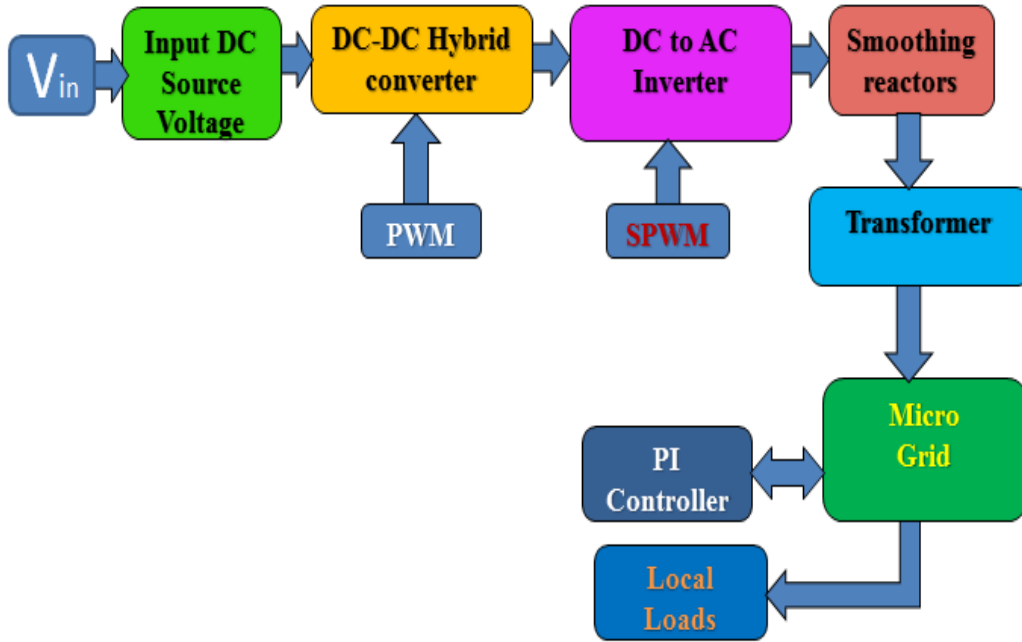


Fig.34 Block diagram for a Novel PV based Single phase 13-level Hybrid H-Bridge inverter fed to R- load

Fig.35 represents the circuit topology for 13-level Hybrid H-Bridge inverter and the respective switching sequence is given in Table 5.

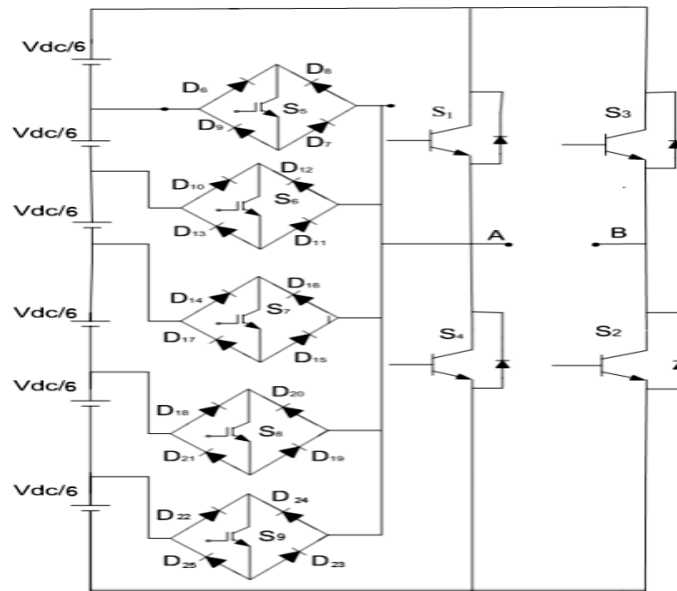


Fig.35 Single phase 13-level Hybrid H-Bridge inverter topology

Table 5: Operating sequence of an inverter

Voltage Level	Switching Operation								
	S <sub>1</sub>	S <sub>2</sub>	S <sub>3</sub>	S <sub>4</sub>	S <sub>5</sub>	S <sub>6</sub>	S <sub>7</sub>	S <sub>8</sub>	S <sub>9</sub>



0	1	0	1	0	0	0	0	0	0
$V_{dc}/6$	0	1	0	0	0	0	0	0	1
$V_{dc}/3$	0	1	0	0	0	0	0	1	0
$V_{dc}/2$	0	1	0	0	0	0	1	0	0
$2V_{dc}/3$	0	1	0	0	0	1	0	0	0
$5V_{dc}/6$	0	1	0	0	1	0	0	0	0
$V_{dc}$	1	1	0	0	0	0	0	0	0
$-V_{dc}/6$	0	0	1	0	1	0	0	0	0
$-V_{dc}/3$	0	0	1	0	0	1	0	0	0
$-V_{dc}/2$	0	0	1	0	0	0	1	0	0
$-2V_{dc}/3$	0	0	1	0	0	0	0	1	0
$-5V_{dc}/6$	0	0	1	0	0	0	0	0	1
$-V_{dc}$	1	0	1	0	0	0	0	0	0

There are 7 modes of switching for different levels from 0 to  $V_{dc}$ . For getting  $V_{dc}/6$  we need to turn on  $S_2$  and  $S_9$  so that O/P voltage across resistor is  $V_{dc}/6$ . Similarly, the operation will continue for the remaining switches as described in table.5

*A. MATLAB/SIMULINK MODEL FOR A NOVEL PV BASED 13-LEVEL HYBRID H-BRIDGE INVERTER FED TO R-LOAD*

Fig.36,37,38 & 39 represents the MATLAB/Simulink model and corresponding, wave forms of the 13-level Hybrid H-Bridge inverter, the O/P wave form of voltage, current and FFT Analysis.

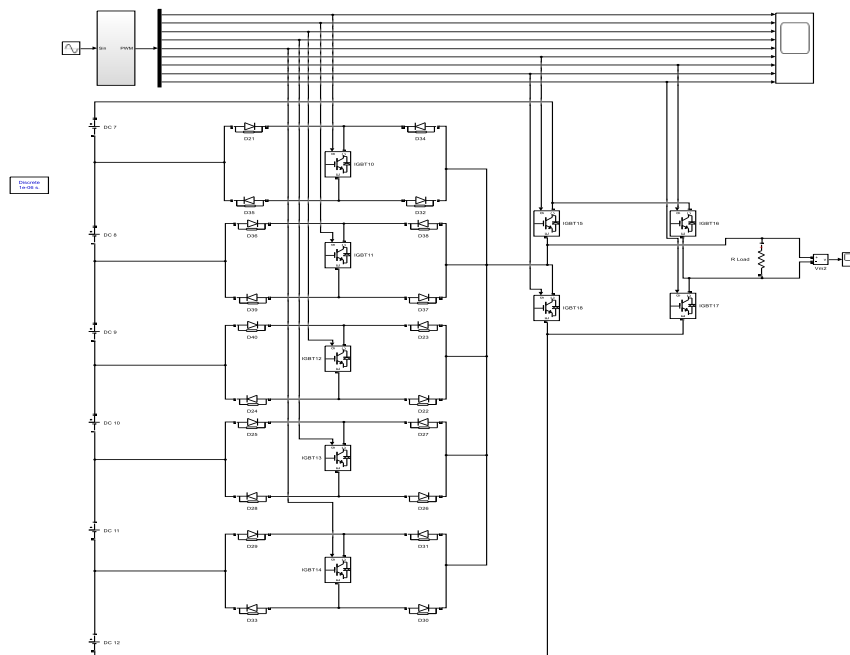


**Fig.36 Single phase 13-level Hybrid H-Bridge inverter fed to constant load**

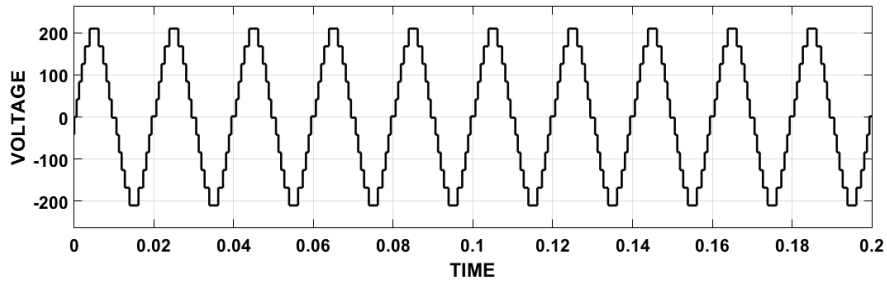


**Fig.37 O/P Voltage wave form of 13-level inverter**

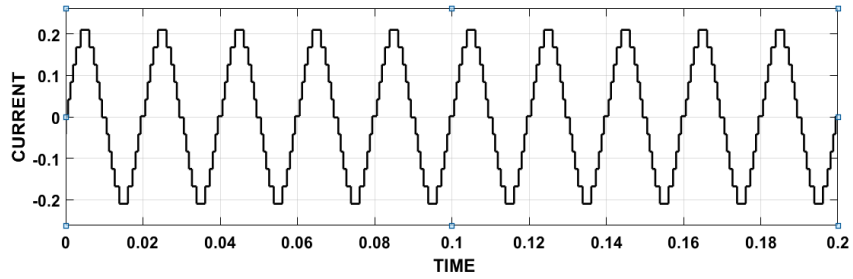


**Fig.38 O/P Current waveform of 13-level inverter**

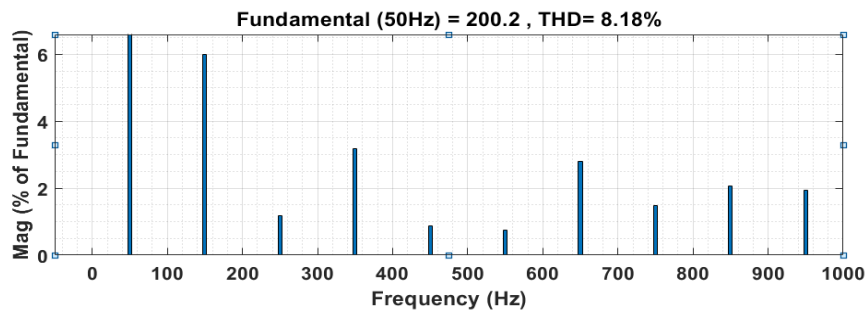


**Fig.39 FFT Analysis for 13-level inverter**

VIII. PROPOSED 21-LEVEL HYBRID H-BRIDGE INVERTER

Proposed 21-level Hybrid H-Bridge inverter, is shown in Fig.40. In this 10 DC voltage supplies are used with  $V_{dc}/10$ .

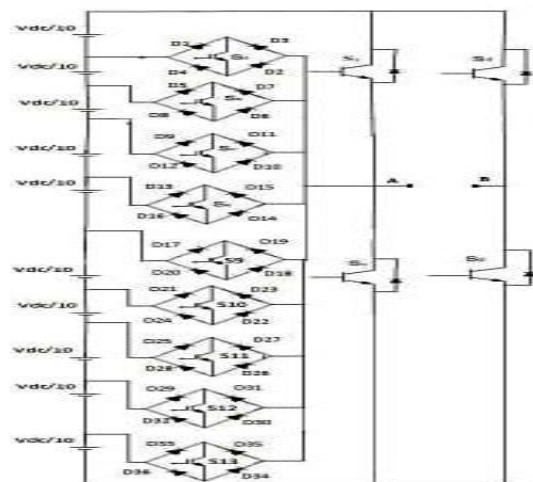


**Fig.40 Proposed 21-level Hybrid H-Bridge inverter topology**

Table 6 gives the switching for proposed 21-level Hybrid H-Bridge Inverter

**Table 6: Operating sequence of an inverter**

Voltage Level	Switching Operation												
	S <sub>1</sub>	S <sub>2</sub>	S <sub>3</sub>	S <sub>4</sub>	S <sub>5</sub>	S <sub>6</sub>	S <sub>7</sub>	S <sub>8</sub>	S <sub>9</sub>	S <sub>10</sub>	S <sub>11</sub>	S <sub>12</sub>	S <sub>13</sub>
0	0	1	0	1	0	0	0	0	0	0	0	0	0
1V <sub>dc</sub> /10	0	1	0	0	0	0	0	0	0	0	0	0	1
2V <sub>dc</sub> /10	0	1	0	0	0	0	0	0	0	0	0	1	0
3V <sub>dc</sub> /10	0	1	0	0	0	0	0	0	0	0	1	0	0
4V <sub>dc</sub> /10	0	1	0	0	0	0	0	0	0	1	0	0	0
5V <sub>dc</sub> /10	0	1	0	0	0	0	0	0	1	0	0	0	0
6V <sub>dc</sub> /10	0	1	0	0	0	0	0	1	0	0	0	0	0
7V <sub>dc</sub> /10	0	1	0	0	0	0	1	0	0	0	0	0	0
8V <sub>dc</sub> /10	0	1	0	0	0	1	0	0	0	0	0	0	0
9V <sub>dc</sub> /10	0	1	0	0	1	0	0	0	0	0	0	0	0
-V <sub>dc</sub>	0	1	0	0	0	0	0	0	0	0	0	0	0
-1V <sub>dc</sub> /10	0	0	1	0	1	0	0	0	0	0	0	0	0
-2V <sub>dc</sub> /10	0	0	1	0	0	1	0	0	0	0	0	0	0
-3V <sub>dc</sub> /10	0	0	1	0	0	0	1	0	0	0	0	0	0
-4V <sub>dc</sub> /10	0	0	1	0	0	0	0	1	0	0	0	0	0
-5V <sub>dc</sub> /10	0	0	1	0	0	0	0	0	1	0	0	0	0
-6V <sub>dc</sub> /10	0	0	1	0	0	0	0	0	0	1	0	0	0
-7V <sub>dc</sub> /10	0	0	1	0	0	0	0	0	0	0	1	0	0
-8V <sub>dc</sub> /10	0	0	1	0	0	0	0	0	0	0	0	1	0
-9V <sub>dc</sub> /10	0	0	1	0	0	0	0	0	0	0	0	0	1
-V <sub>dc</sub>	0	0	1	1	0	0	0	0	0	0	0	0	0

Table 10 gives modes of switching for different levels from 0 to 9V<sub>dc</sub>/10. For getting 1V<sub>dc</sub>/10, need to turn on S<sub>2</sub> and S<sub>13</sub> so that O/P voltage across resistor is 1V<sub>dc</sub>/10. Similarly, the operation will continue for the remaining switches as described in Table 6.

*A. MATLAB/Simulink model for proposed 21-level Hybrid H-Bridge inverter fed to R- Load*

Fig.41,42,43&44. represents the MATLAB/Simulink model and corresponding wave forms of the 21-level Hybrid H-Bridge inverter, the O/P wave form of voltage, current and FFT Analysis.

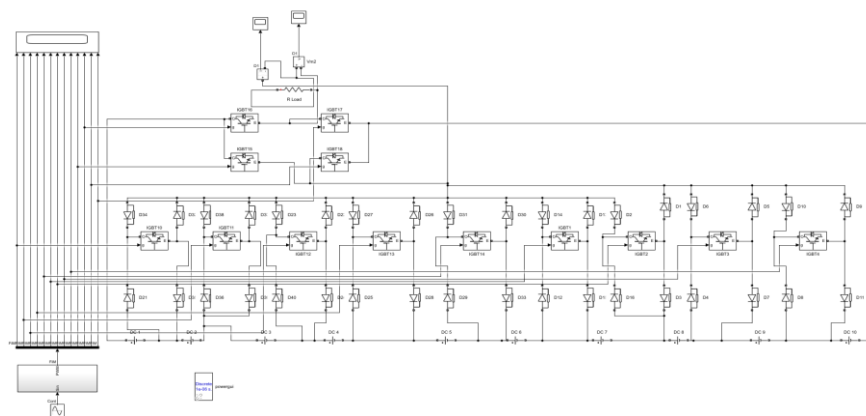


**Fig.41 The proposed 21-level Hybrid H-Bridge inverter fed to R-load**

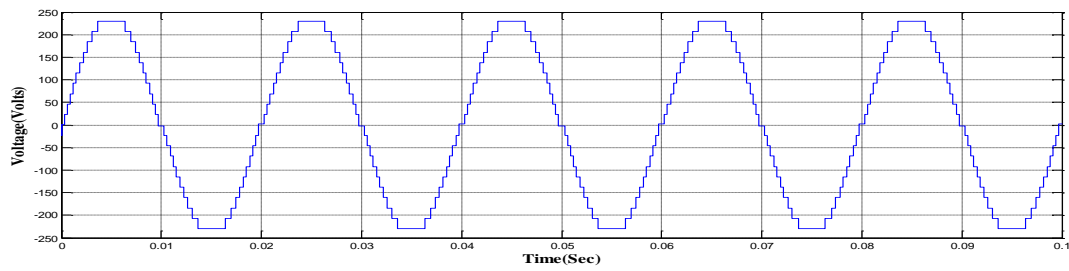


**Fig.42 O/P Voltage for 21-level Hybrid inverter**

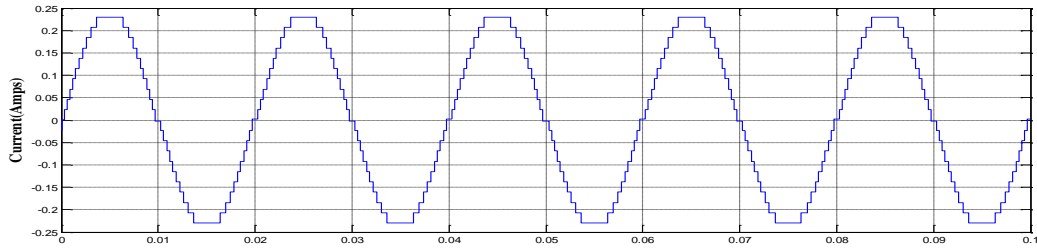


**Fig.43 O/P Current for 21-level hybrid inverter**

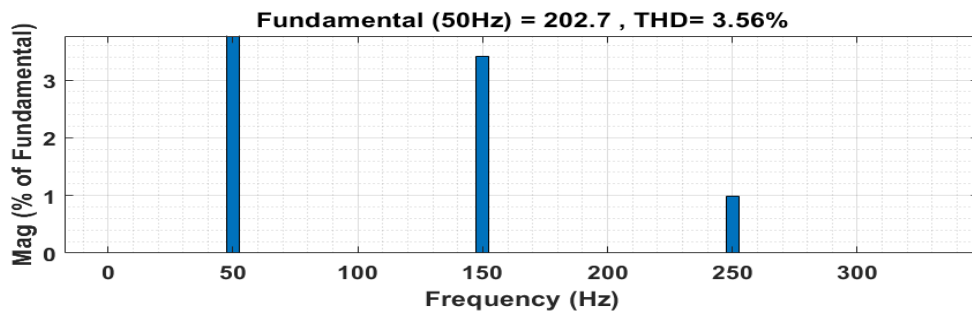


**Fig.44 FFT analysis for 21-level Hybrid H-Bridge inverter**

**Table -7 Comparison of proposed topology with conventional topologies**

S.NO	PARAMETERS	CONVENTIONAL CHB-11 LEVEL [3]	CONVENTIONAL CHB-13 LEVEL [2]	CONVENTIONAL CHB-21 LEVEL [2&10]	Hybrid H-Bridge inverter -13 LEVEL	PROPOSED Hybrid H-Bridge inverter -21 LEVEL
1	No.of switches	20	28	40	9	13
2	No.of dc Supply voltages	5	7	10	6	9
3	Load resistance	1k	1k	1K	1k	1k
4	Input voltage	210	250	240	252	260
5	Output voltage	200	209	223	210	208
6	OutPut current	0.200	0.209	0.223	0.210	0.208

7	Total THD%	20.08	12.80	9.66	8.18	3.56
---	------------	-------	-------	------	------	------

### Conclusion

It is observed that the presented novel hybrid DC-DC boost converter is giving reduced ripple content in the O/P voltage when compared with normal boost converter. The O/P of this boost converter is fed to the proposed inverter topologies. Cascaded 11 & 13-level inverters are also presented in this paper. Based on the results, it is observed that with an increase in level of voltage, the THD is reducing, and O/P voltage efficiency is improved. On the other hand, the number of switches also increases which results in high losses with low efficiency. This problem can be resolved with the help of a proposed 13-level and 21-level inverter configuration. It involves 10 switches for getting 13 level single stage voltages while the ordinary CHB requires 24 switches for similar degree of 13 level voltages. The proposed multi-level inverter can be utilized as a drive for solar oriented controlled applications. A closed loop control can be created utilizing clever calculations to upgrade the exchanging point. The planning and execution of additional levels might diminish the THD to a lesser value and thereby overcome the existing problems of multilevel inverters. Thus, from the above presented results, it is concluded that, the present novel configuration converter gives low THD and improved efficiency with a reduced number of switches. These models are used in micro grid applications, because it requires an efficient converter with low cost and less design complexity.

### REFERENCES

- [1] George, Jibin, and Anish Benny. "Real-time harmonic minimization of multilevel inverters used in photovoltaic systems." In 2013 Fourth International Conference on Computing, Communications and Networking Technologies (ICCCNT), pp.1-6. IEEE, 2013.
- [2] Shuvo, Shuvangkar, EklasHossain, Tanveerul Islam, AbirAkib, Sanjeevikumar Padmanaban, and MdZiaurRahman Khan. "Design and hardware implementation considerations of modified multilevel cascaded H-bridge inverter for photovoltaic system." IEEE Access 7 (2019): 16504-16524.
- [3] Sekhar, Punya, PV Ramana Rao, and M. Uma Vani. "Novel multilevel inverter with minimum number of switches." In 2017 International Conference on Recent Trends in Electrical, Electronics and Computing Technologies (ICRTEECT), pp. 106-112. IEEE, 2017.
- [4] Gaikwad, Asha, and Pallavi Appaso Arbune. "Study of cascaded H-Bridge multilevel inverter." In 2016 international conference on automatic control and dynamic optimization techniques (ICACDOT), pp. 179-182. IEEE, 2016.
- [5] Gupta, Krishna Kumar, and Pallavee Bhatnagar. Multilevel inverters: conventional and emerging topologies and their control. Academic Press, 2017.
- [6] Chinnaiyan, Venkatachalam Kumar, Jovitha Jerome, and J. Karpagam. "An experimental investigation on a multilevel inverter for solar energy applications." International Journal of Electrical Power & Energy Systems 47 (2013): 157-167.
- [7] Guo, Xiaoqiang, Ran He, and Mehdi Narimani. "Modeling and analysis of new multilevel inverter for solar photovoltaic power plant." International Journal of Photoenergy 2016.
- [8] Khoukha, Imarazene, Chekireb Hachemi, and Berkouk El Madjid. "Multilevel selective harmonic elimination PWM technique in the nine level voltage inverter." In 2007 International Conference on Computer Engineering & Systems, pp. 387-392. IEEE, 2007.
- [9] Latha, J. Hema, and Basava Raja Banakara. "Modeling and analysis of 21 level cascade model multilevel inverter." In 2018 2nd International Conference on Inventive Systems and Control , pp. 586-591. IEEE, 2018.
- [10] R. Bauwels Gonzatti, Y. Li, M. Amirabadi, B. Lehman and F. Z. Peng, "An Overview of Converter Topologies and their derivations and Interrelationships," in IEEE Journal of Emerging and Selected Topics in Power Electronics, Vol. 10, No. 6, pp. 6417-6429, Dec. 2022, doi: 10.1109/JESTPE.2022.3181217.
- [11] Devulal, B., M. Siva, D. Ravi Kumar, and V. Rajashekar. "Design and Analysis of Micro-grid Stability with Various DGs." In International Conference on Electrical and Electronics Engineering, pp. 406-414. Singapore: Springer Nature Singapore, 2022.

- [12] JyotiSastry a Panagiotis Bakas b, Hongrae Kim a, Lei Wang c, Antonios Marinopoulos "Evaluation of cascaded H-bridge inverter for utility-scale photovoltaic systems" ABB, Corporate Research, Raleigh, NC 27606, USA ABB AB, Corporate Research, Power Technologies, Västerås SE 72178, Sweden ABBInc,
- [13] Bailu Xiao , Lijun Hang1, Jun Mei , Cameron Riley , Leon M. Tolbert, Burak Ozpineci "Modular Cascaded H-Bridge Multilevel PV Inverter with Distributed MPPT for Grid-Connected Applications" IEEE Xplore: 13 Nov 2014 Electronic ISBN:978-1-4799-5776-7
- [14] Verma, Akash Deep, Anuradha Tomar, and Prerna Gaur. "Design and Assessment of Unified Multi-Input Multi-Output Converter Based Islanded Microgrid for Rural and Remote Areas." Electric Power Components and Systems (2023): 1-18.